Zinc transporter Znt5/Slc30a5 is required for the mast cell–mediated delayed-type allergic reaction but not the immediate-type reaction

Keigo Nishida,[1,2] Aiko Hasegawa,[1,3] Susumu Nakae,[4,5,6] Keisuke Oboki,[4,5] Hirohisa Saito,[4,5] Satoru Yamasaki,[1] and Toshio Hirano[1,3]

[1]Laboratory for Cytokine Signaling, RIKEN Research Center for Allergy and Immunology, Yokohama, Kanagawa 230-0045, Japan
[2]Immune system, Cooperation Program, Graduate School of Frontier Biosciences, Osaka University, Osaka 565-0871, Japan
[3]Laboratory of Developmental Immunology and the Core Research for Evolutional Science and Technology Program (CREST) of the Japan Science and Technology Agency, Graduate School of Frontier Biosciences, Graduate School of Medicine, and WPI Immunology Frontier Research Center, Osaka University, Osaka 565-0817, Japan
[4]Department of Allergy and Immunology, National Research Institute for Child Health and Development, Tokyo 157-8535, Japan
[5]Atopy Research Center, Juntendo University, Tokyo 113-8421, Japan
[6]Frontier Research Initiative, Institute of Medical Science, University of Tokyo, Tokyo 108-8639, Japan

Zinc (Zn) is an essential nutrient and its deficiency causes immunodeficiency. However, it remains unknown how Zn homeostasis is regulated in mast cells and if Zn transporters are involved in allergic reactions. We show that Znt5/Slc30a5 is required for contact hypersensitivity and mast cell–mediated delayed-type allergic response but not for immediate passive cutaneous anaphylaxis. In mast cells from Znt5$^{-/-}$ mice, Fcε receptor I (FcεRI)–induced cytokine production was diminished, but degranulation was intact. Znt5 was involved in FcεRI-induced translocation of protein kinase C (PKC) to the plasma membrane and the nuclear translocation of nuclear factor κB. In addition, the Zn finger–like motif of PKC was required for its plasma membrane translocation and binding to diacylglycerol. Thus, Znt5 is selectively required for the mast cell–mediated delayed-type allergic response, and it is a novel player in mast cell activation.

CORRESPONDENCE
Toshio Hirano:
hirano@
molonc.med.osaka-u.ac.jp

Abbreviations used: BMMC, BM-derived mast cell; cDNA, complementary DNA; CHS, contact hypersensitivity; DAG, diacylglycerol; ERK, extracellular signal-regulated kinase; FcεRI, Fcε receptor I; MAPK, mitogen-activated protein kinase; mRNA, messenger RNA; PCA, passive cutaneous anaphylaxis; PKC, protein kinase C; PVDF, polyvinylidine fluoride; Slc, solute-linked carrier; Zip, ZRT/IRT-related protein; Zn, zinc; Znt, Zn transporter.

Zinc (Zn) is one of the essential trace elements. It is a structural component of a great number of proteins, including enzymes and transcription factors, and it is essential for their biological activity (1, 2). Zn has a variety of effects in the immune system (3). Zn-deficient mice have defects in natural killer cell–mediated cytotoxic activity, antibody-mediated responses, host defense against pathogens, and tumors (4–6). In contrast, Zn itself is cytotoxic, and it induces apoptosis in T and B cells (7). Therefore, cells have evolved a complex system to maintain a balance of Zn uptake, intracellular storage, and efflux (8–11). Two solute-linked carrier (Slc) protein families have been identified in Zn transport: the Zn transporter (Znt)/Slc30 and ZRT/IRT-related protein (Zip)/Slc39 (8, 11–13). Znt transporters reduce cytoplasmic Zn availability by promoting Zn efflux from the cytoplasm into the extracellular space or intracellular compartments. The Zip transporters increase cytoplasmic Zn availability by promoting extracellular Zn uptake and Zn release from compartments into the cytoplasm.

Zn has also been implicated as an intracellular signaling molecule (14–17). A nematode ZnT1 orthologue, CDF1, positively affects Ras–extracellular signal-regulated kinase (ERK) signal transduction (18). Slc39a7/Zip7 was found to affect epidermal growth factor/insulin-like growth factor signaling and tamoxifen resistance of breast cancer cells (19). We showed that Slc39a6/Zip6/Liv1 controls the nuclear localization of the Zn finger transcription factor Snail (20). In addition, Toll-like receptor 4–mediated DC maturation is, at least in part, dependent on a Toll-like receptor 4–induced decrease in intracellular free Zn effected by a change in the gene expression profile of Zip

K. Nishida and A. Hasegawa contributed equally to this paper.

The Rockefeller University Press $30.00
J. Exp. Med. Vol. 206 No. 6 1351-1364
www.jem.org/cgi/doi/10.1084/jem.20082533

and Znt family members (21). Furthermore, in mast cells, Fcε receptor I (FcεRI) stimulation induces an increase in intracellular free Zn, a phenomenon called the "Zn wave" (22). These results support the idea that Zn is involved in intracellular signaling and lead to the prediction that Znts have roles not only in maintaining Zn homeostasis but also in intracellular signaling events (17). Along these lines, we previously showed that Zn might be required for mast cell activation in allergic responses; the Zn chelator TPEN (*N*,*N*,*N*,*N*-tetrakis (2-pyridylmethyl) ethylenediamine) inhibits FcεRI-mediated NF-κB activation and degranulation in mast cells (23). All of these results suggest that Zn has pivotal roles in mast cell function. However, it remains completely unknown how Zn homeostasis is regulated in mast cells and if Znts are involved in mast cell function.

Mast cells are major players in allergy responses such as immediate- and delayed-type hypersensitivity reactions (24–26). Passive cutaneous anaphylaxis (PCA) and contact hypersensitivity (CHS) are mouse models for in vivo immediate-type and delayed-type reactions, respectively (27–29). FcεRI stimulation activates several downstream pathways that initiate the allergic inflammatory process by eliciting mast cell degranulation accompanied by the rapid release of preformed chemical mediators such as histamine and serotonin. This process plays critical roles in the immediate-type allergic response. In contrast, the mast cell–mediated delayed responses and IgE-induced chronic allergic inflammatory processes are mainly dependent on cytokine production (30, 31). One important question in mast cell biology is how the early signaling events after FcεRI stimulation are integrated and how specific mast cell responses, such as immediate degranulation versus a delayed-type allergic reaction, are selected. It would be helpful to understand these mechanisms because the identification of molecules that selectively regulate specific mast cell effector functions could provide targets for therapies for mast cell–mediated diseases.

FcεRI stimulation can induce the de novo synthesis of proinflammatory cytokines such as IL-6 and TNF-α (32, 33). In particular, both calcium and diacylglycerol (DAG) activate conventional protein kinase C (PKC) isoforms that mediate a critical positive signal necessary for cytokine production in mast cells (34, 35). In addition, conventional PKCs have two regions in their regulatory domain, C1 and C2, in common. The C1 region regulates the activation or translocation of PKC and has two cysteine-rich loops (Zn finger-like motifs) that interact with DAG or phorbol esters (36–40). The C2 region mediates calcium binding. Recently, in T, B, and mast cells, PKCs were shown to be important for NF-κB activation and the upstream function of an adaptor protein complex composed of Bcl-10 and MALT1 (41–43). Collectively, these studies indicate that the PKC/Bcl-10/MALT1/NF-κB cascade plays important roles in cytokine production. Although this linear cascade is well established, it still seems oversimplified. Additional molecules are likely to be involved in the regulation of the PKC–NF-κB signaling pathway.

Inoue et al. (44) reported that mice deficient in Znt5 show severe osteopenia and male-specific sudden death from bradyarrhythmia during their reproductive period. We demonstrate in this paper that a Znt, Znt5, is required for the mast cell–mediated delayed-type allergic response but not the immediate response. Znt5 is required for the FcεRI-induced translocation of PKC-β to the plasma membrane and, therefore, for NF-κB–dependent cytokine production. These observations provide the first genetic evidence that a Znt, Znt5, is required for immunological responses and has a selective role in allergic reactions.

RESULTS

Znt5 is highly expressed in BM-derived mast cells (BMMCs) but not required for mast cell development

There are eight known members of the Znt family (45). To examine the role of the Znts in mast cells, we checked the expression level of each family member in BMMCs by examining the ReFDIC (Reference Database of Immune Cells) (46). The database showed that Znt5 was among the Znts that were highly expressed in BMMCs (Fig. S1). The messenger RNA (mRNA) level of Znt5 was also enhanced by FcεRI stimulation (Fig. 1 A and Fig. S2). Because $Znt5^{-/-}$ mice are available (44), we focused on Znt5 to clarify its role in mast cell function. First, we determined that Znt5 protein was expressed in BMMCs from WT but not $Znt5^{-/-}$ mice (Fig. 1 B). We also determined that in the BMMCs, Znt5 was mainly located in the Golgi (Fig. 1 C), as reported previously for other cell types (47, 48). Next, we investigated whether Zn homeostasis was disordered in $Znt5^{-/-}$ mast cells using a cell-permeable Zn-specific fluorescent probe, Newport green DCF diacetate, which predominantly localizes to the cytoplasm. The $Znt5^{-/-}$ BMMCs showed an increased level of free Zn in the cytoplasm ($Znt5^{+/+} = 0.0723 \pm 0.00225$ μM; $Znt5^{-/-} = 0.106 \pm 0.0132$ μM; $P < 0.05$; Fig. 1 D), indicating that the intracellular distribution of free Zn was impaired in the $Znt5^{-/-}$ BMMCs.

We next asked if Znt5 was required for mast cell development. Culturing BM cells from WT and $Znt5^{-/-}$ mice in the presence of IL-3 yielded highly purified mast cell populations. These BMMCs, whether derived from WT or $Znt5^{-/-}$ mice, were indistinguishable in morphology when stained with Alcian blue (Fig. S3 A). The growth rate and total cell numbers in these cultures, as well as the frequency of BMMCs as revealed by flow cytometric analysis of the surface expression of c-kit and FcεRI, were equivalent (Fig. S3 B). In addition to the normal in vitro development of the mast cells, the number of mast cells, their morphology, and their anatomical distribution in the ear, skin, and stomach of WT and $Znt5^{-/-}$ mice were comparable (Fig. S4, A and B). Collectively, these findings demonstrated that Znt5 is not required for mast cell development.

Znt5 is selectively required for the CHS but not the PCA reaction

We examined the roles played by Znt5 in vivo in PCA and CHS using the $Znt5^{-/-}$ mice. We first tested the importance of Znt5 in the PCA model by evaluating the extravasation of

Evans blue dye in the ears of mice that had been sensitized and challenged with an antigen. However, there was no notable difference in the extravasation kinetics or total amount of Evans blue dye in the ear in the WT and Znt5$^{-/-}$ mice (Fig. 2 A), indicating that the mast cell–mediated PCA reaction occurs normally in the absence of Znt5.

We next examined the CHS response, which is promoted by mast cell–derived proinflammatory cytokines. WT mice developed robust CHS responses to experimental hapten such as FITC, as assessed by tissue swelling at the site of hapten challenge, which reached a maximum 24 h after antigen stimulation (Fig. 2 B). Consistent with a previous study (31), mast cell–deficient *Kit*$^{W\text{-}sh/W\text{-}sh}$ mice developed a low-level FITC-induced CHS reaction (Fig. 2 B). The Znt5$^{-/-}$ mice exhibited a similar defective CHS reaction (Fig. 2 B). Even 24 h after the antigen challenge, the increase in ear thickness of the Znt5$^{-/-}$ mice was <45% of that of WT mice. Consistent with this result, the affected ear of the Znt5$^{-/-}$ mice showed significantly reduced FITC-induced cytokine production and transcription of the genes for IL-6, IL-1β, MCP, and TNF-α (Fig. 2, C and D). The Znt5$^{-/-}$ ears also showed a decrease in the transcription level of the genes for chemokines such as MIP-2 (CXCL2; Fig. 2 C). From these results, we concluded that Znt5 was selectively required for CHS, but not for PCA, in vivo. To determine whether defectiveness in CHS response in Znt5$^{-/-}$ mice is caused by the lack of Znt5 in mast cell but not in other environmental cells and tissues, we checked *Kit*$^{W\text{-}sh/W\text{-}sh}$ mice that had been engrafted with mast cell from either WT or Znt5$^{-/-}$ mice. We found that engraftment with BMMCs from WT mice, but not Znt5$^{-/-}$ mice, restored CHS response in *Kit*$^{W\text{-}sh/W\text{-}sh}$ mice (Fig. 2 E). Consistent with these results, *Kit*$^{W\text{-}sh/W\text{-}sh}$ mice reconstituted with Znt5$^{-/-}$ BMMCs had significantly reduced FITC-induced cytokine expression level such as TNF-α and IL-6 in the ear (Fig. 2 F). The number of mast cells per mm^2 of dermis did not change between Znt5$^{+/+}$ and Znt5$^{-/-}$ BMMC-engrafted *Kit*$^{W\text{-}sh/W\text{-}sh}$ mice (Fig. S5). Collectively, these findings showed that Znt5 in mast cells is required for FITC-induced CHS responses.

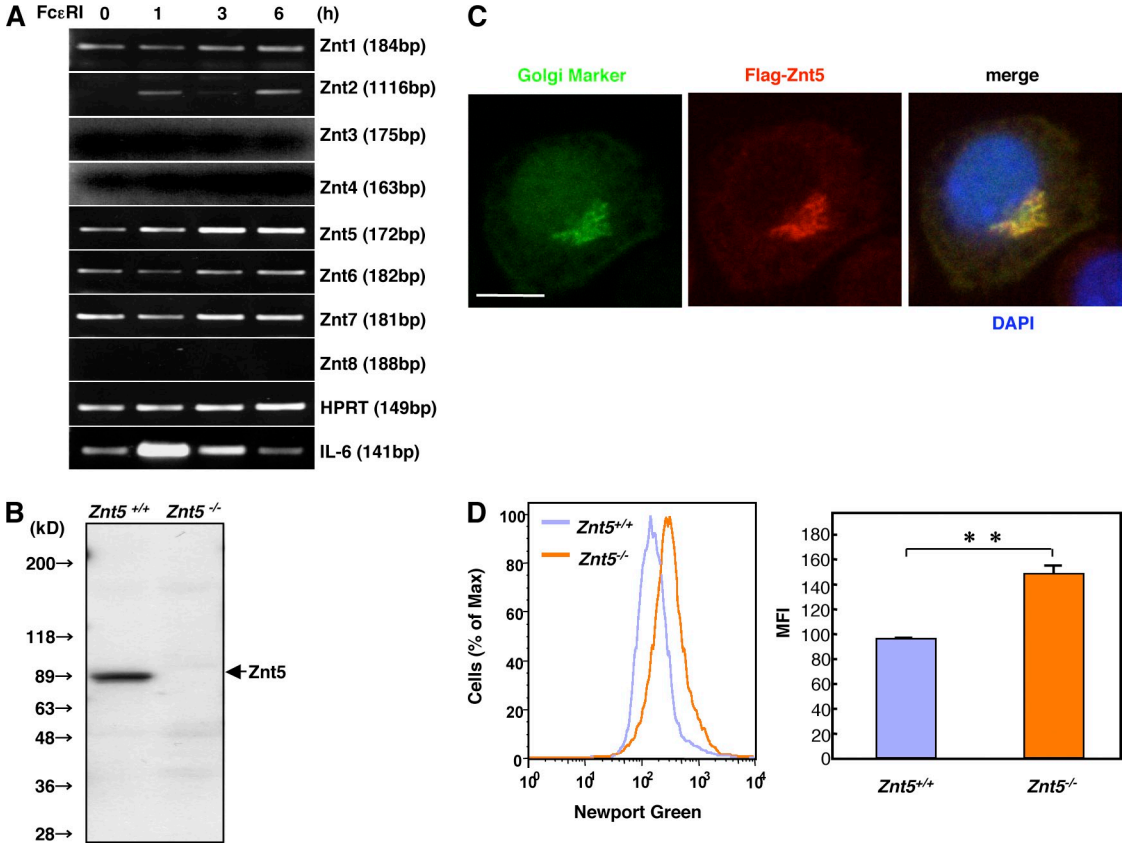

Figure 1. Localization of Znt5 in BMMCs. (A) RT-PCR of mRNAs encoding Znt family members (1–8), IL-6, and hypoxanthine-guanine phosphoribosyl transferase in BMMCs. BMMCs were untreated or treated with DNP–human serum albumin (HSA) for the indicated times. (B) Immunoblotting analysis of Znt5 in BMMCs. The BMMCs from Znt5$^{+/+}$ and Znt5$^{-/-}$ mice were analyzed by immunoblotting with an anti-Znt5 antibody. (C) Subcellular localization of ectopically expressed Flag-hZnt5 in BMMCs. Cells were retrovirally transfected with Flag-hZnt5 (described in Materials and methods), and then cells were double stained with FITC-conjugated anti-GM130 antibody (green) and Zenon-conjugated anti-flag antibody (red). Nuclei were labeled with DAPI (blue). Bar, 5 µm. (D) FACS analysis of intracellular free Zn using a Zn indicator, Newport green (left). Blue line, BMMCs from Znt5$^{+/+}$ mice; orange line, BMMCs from Znt5$^{-/-}$ mice. Histograms show mean fluorescent intensity (right). Data show mean + SD. **, P < 0.01 (two-tailed Student's *t* test). A representative dataset of the three (A, C, and D) or two (B) experiments performed, each of which gave similar results, is shown.

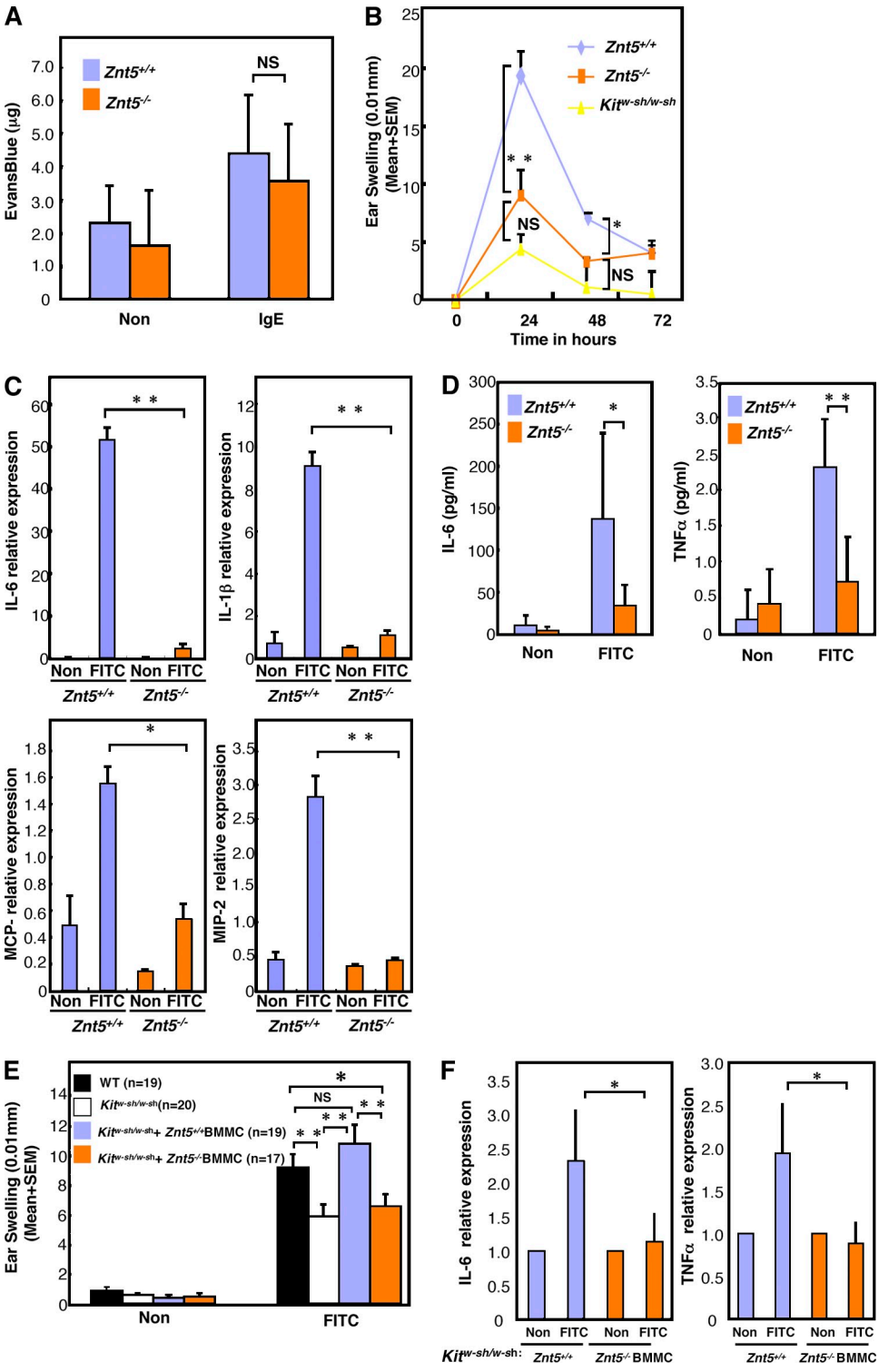

Figure 2. Normal PCA but defective CHS response in Znt5$^{-/-}$ mice. (A) Analysis of PCA in Znt5$^{+/+}$ mice (n = 12) and Znt5$^{-/-}$ mice (n = 11) that received intradermal injections of IgE anti-DNP into the right ear and of saline into the left ear (control, non). After sensitization, mice were intravenously challenged with DNP-BSA. Data show mean + SD of the extravasation of Evans blue into the ears. (B) Analysis of the CHS response in Znt5$^{+/+}$ (n = 14), Znt5$^{-/-}$ (n = 14), and *Kit*$^{W\text{-}sh/W\text{-}sh}$ (n = 11) mice. Znt5$^{+/+}$, Znt5$^{-/-}$, and *Kit*$^{W\text{-}sh/W\text{-}sh}$ mice were sensitized with FITC. Ear swelling was measured at the indicated times after hapten challenge. Data show mean + SEM. (C) Real-time quantitative RT-PCR of mRNAs for cytokines, chemokines, and GAPDH (loading control) expressed in the ears of Znt5$^{+/-}$ and Znt5$^{-/-}$ mice challenged with FITC after 6 h. Data show the mean + SD (n = 3 per group). (D) Concentrations of IL-6 and TNF-α in Znt5$^{+/+}$ (IL-6, n = 10; TNF-α, n = 5) and Znt5$^{-/-}$ (IL-6, n = 10; TNF-α, n = 5) mice challenged with FITC and measured by enzyme-

Znt5 is required for FcεRI-mediated cytokine production but not for degranulation in BMMCs

FcεRI-induced degranulation and the production of lipid mediators play crucial roles in the PCA reaction, whereas cytokine production is essential for the CHS response (49). To learn the basis for the selective defect in the CHS reaction of Znt5$^{-/-}$ mice, we examined the capacities of Znt5$^{-/-}$ BMMCs to degranulate, synthesize, and secrete lipid mediators and to produce cytokines. BMMCs derived from Znt5$^{-/-}$ mice released similar amounts of β-hexosaminidase to WT BMMCs in response to FcεRI stimulation (Fig. 3 A), indicating that their ability to degranulate was intact. Furthermore, FcεRI stimulation-induced lipid mediator secretion, such as that of leukotrienes C_4, occurred normally in the Znt5$^{-/-}$ BMMCs (Fig. 3 B). These results were consistent with the normal PCA reaction observed in the Znt5$^{-/-}$ mice. However, the production of the FcεRI-induced cytokines IL-6 and TNF-α was significantly reduced in Znt5$^{-/-}$ BMMCs as compared with WT BMMCs (Fig. 3 C). Furthermore, PMA-induced cytokine production was also diminished in Znt5$^{-/-}$ BMMCs (Fig. 3 D). To rule out the possibility that the defect in cytokine production was caused by an impaired cytokine transport step in Znt5$^{-/-}$ BMMCs, we checked the ability of LPS to induce cytokine production. As shown in Fig. 3 E, the LPS-induced production of the cytokines IL-6 and TNF-α did not decrease in the Znt5$^{-/-}$ BMMCs. These results indicated that Znt5 is selectively required for FcεRI-induced cytokine production but not for degranulation in BMMCs.

Znt5 is involved in FcεRI-mediated NF-κB signaling

To define the molecular mechanisms responsible for the defective cytokine production in Znt5$^{-/-}$ BMMCs, we analyzed the cytokine mRNA levels using quantitative PCR. The FcεRI stimulation of BMMCs led to a time-dependent increase in the IL-6 and TNF-α mRNA level. However, the level of IL-6 and TNF-α mRNA that was induced was significantly lower in the Znt5$^{-/-}$ BMMCs (Fig. 4 A). As expected from the result shown in Fig. 3 E, the levels of LPS-induced IL-6 and TNF-α mRNA in the Znt5$^{-/-}$ BMMCs were not decreased as compared with those in WT (Fig. 4 B). Thus, Znt5 contributed to the FcεRI-induced increase of mRNA for IL-6 and TNF-α.

We further analyzed whether Znt5 was involved in the FcεRI-induced nuclear translocation of NF-κB. As shown in Fig. 4 C, the FcεRI-induced translocation of p65 to the nucleus was significantly decreased in the Znt5$^{-/-}$ BMMCs. Consistent with these results, FcεRI-mediated IκBα phosphorylation and its subsequent degradation were impaired in the Znt5$^{-/-}$ BMMCs (Fig. 4 D and Fig. S6). In contrast, the FcεRI-induced activation of the mitogen-activated protein kinases (MAPKs) ERK1/2, JNK1/2, and p38 was not diminished in the Znt5$^{-/-}$ BMMCs (Fig. 4 E). We also investigated whether Znt5 was involved in FcεRI-induced calcium-elicited signaling events. We monitored the tyrosine phosphorylation of LAT and PLC-γ1, which contributed calcium signaling (26, 50). As expected from the result shown in Fig. 3 A, LAT and PLC-γ1 tyrosine phosphorylation was apparently normal in Znt5$^{-/-}$ BMMCs, as was the FcεRI-induced calcium influx (Fig. S7, A and B). Collectively, these results show that Znt5 was selectively required for FcεRI-mediated NF-κB activation in BMMCs.

Znt5 is required for FcεRI-mediated translocation of PKC-β to the plasma membrane

Because IκBα phosphorylation decreased in Znt5$^{-/-}$ BMMCs (Fig. 4 D and Fig. S6), we next sought to identify the upstream target of Znt5 that was involved in NF-κB activation. Because FcεRI-induced NF-κB activation is dependent on PKC activation (23, 51), we examined the effect of Znt5 on the translocation of PKC to the plasma membrane, a process important for PKC function. As shown in Fig. 5 (A and B), the FcεRI-induced plasma membrane translocation of PKC-β was diminished in the Znt5$^{-/-}$ BMMCs, as was the PMA-induced plasma membrane translocation of PKC-β, and a similar result was obtained in the case of plasma membrane translocation of PKC-α (not depicted). In addition, activity of PKC was reduced in the Znt5$^{-/-}$ BMMCs compared with that in Znt5$^{+/+}$ BMMCs (Fig. S8). Furthermore, we confirmed that transfected Znt5 complementary DNA (cDNA) into the Znt5$^{-/-}$ BMMCs rescued the defect in FcεRI-induced plasma membrane translocation of PKC-β (Fig. 5 C). To rule out the possibility that Znt5 altered the PKC-β expression level, we checked the protein level after FcεRI stimulation and did not find any decrease compared with the level in WT BMMCs (Fig. S9). Together, these results showed that Znt5 is required for the FcεRI-mediated translocation of PKC-β to the plasma membrane and that this effect on PKC-β translocation is, at least in part, the mechanism underlying involvement of Znt5 in FcεRI-induced NF-κB activation, which results in cytokine production.

Zn finger–like motif of PKC-β is important for the PMA-induced plasma membrane translocation of PKC-β

To understand the mechanisms by which Znt5 is involved in the plasma membrane translocation of PKC, we focused on

linked immunosorbent assay. Data show mean + SD. (E) Tissue swelling response to vehicle or FITC in FITC-sensitized C57BL/6 WT mice ($n = 19$), $Kit^{W\text{-}sh/W\text{-}sh}$ mice ($n = 20$), and $Kit^{W\text{-}sh/W\text{-}sh}$ mice that had been selectively repaired of their mast cell deficiency by the intradermal injection of Znt5$^{+/+}$ ($n = 19$) or Znt5$^{-/-}$ ($n = 17$) BMMCs. Data show mean + SEM. (F) Cytokine response to vehicle or FITC in $Kit^{W\text{-}sh/W\text{-}sh}$ mice that had been selectively repaired of their mast cell deficiency by the intradermal injection of Znt5$^{+/+}$ or Znt5$^{-/-}$ BMMCs. TNF-α and IL-6 expression level were measured by real-time quantitative RT-PCR. The expression level of nonstimulation was set as 1. Data show the mean + SD ($n = 4$ per group). *, $P < 0.05$; **, $P < 0.01$. (two-tailed Student's t test). Data are from at least two independent experiments with similar results, with two to six (A and B), three (C), two to five (D), seven to ten (E), or four (F) mice per group per experiment.

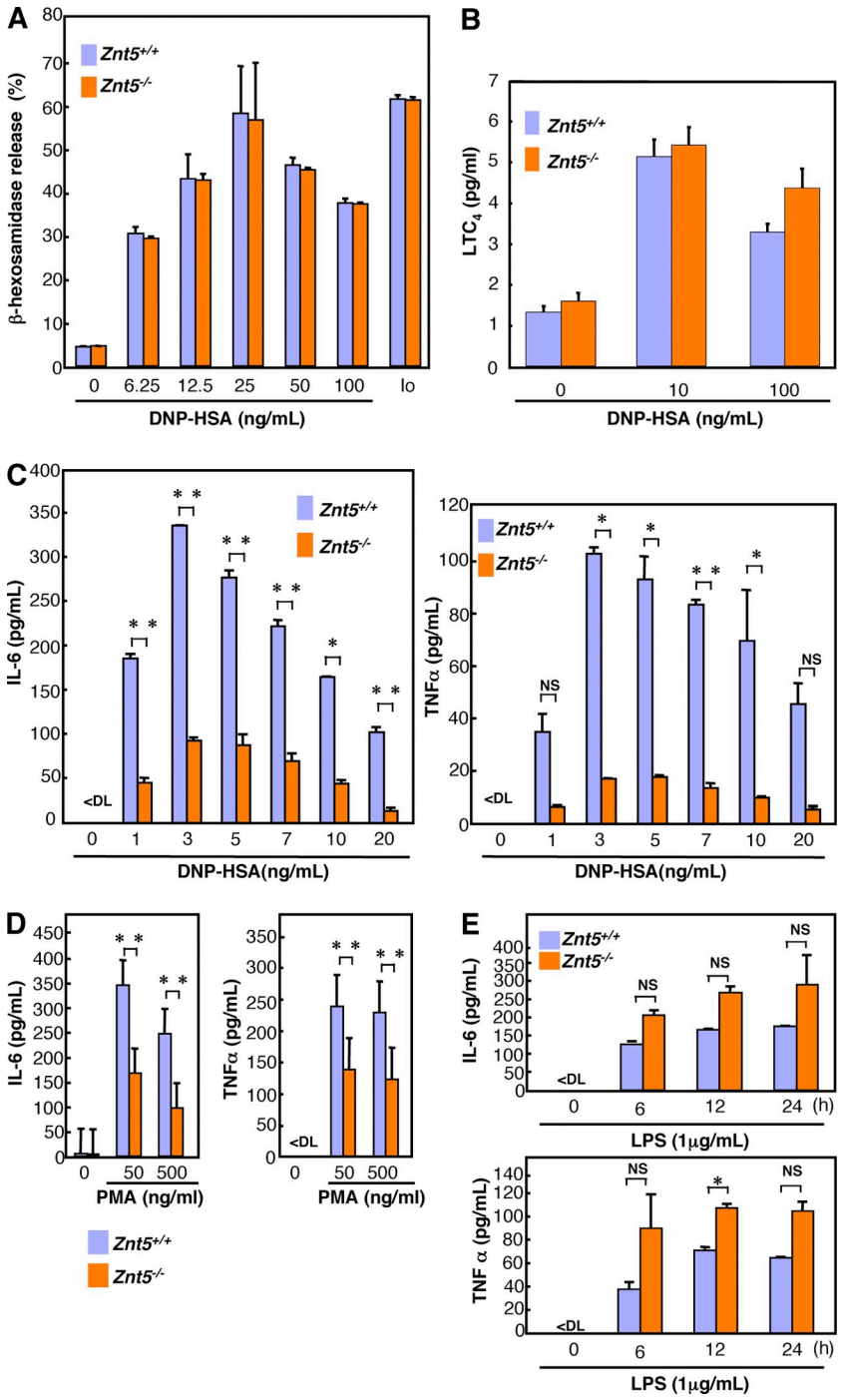

Figure 3. Defective cytokine production in Znt5$^{-/-}$ BMMCs. (A) Degranulation of Znt5$^{+/+}$ and Znt5$^{-/-}$ BMMCs assessed as the release of β-hexosaminidase. BMMCs from Znt5$^{+/+}$ and Znt5$^{-/-}$ mice were sensitized with anti-DNP IgE and stimulated with the indicated concentrations of DNP–HSA. As a control, BMMCs were stimulated with 1 μM ionomycin (Io). Data are the mean + SD. (B) Leukotriene synthesis in Znt5$^{+/+}$ and Znt5$^{-/-}$ BMMCs. Anti-DNP IgE-sensitized BMMCs from the two genotypes were stimulated with DNP–HSA at the indicated concentrations. Leukotrienes C_4 was measured by enzyme-linked immunosorbent assay. Data show the mean + SD. (C) Enzyme-linked immunosorbent assay of IL-6 and TNF-α in BMMCs from Znt5$^{+/+}$ and Znt5$^{-/-}$ mice sensitized with anti-DNP IgE and stimulated with the indicated concentrations of DNP–HSA. Data show the mean + SD. (D) PMA-induced cytokine production in Znt5$^{+/+}$ and Znt5$^{-/-}$ BMMCs stimulated with 50 and 500 ng/ml PMA. Data show the mean + SD. (E) LPS-induced cytokine production in Znt5$^{+/+}$ and Znt5$^{-/-}$ BMMCs stimulated with 1 μg/ml LPS for the indicated time. <DL, below detection limit. Data show the mean + SD. A representative dataset of the five (A), four (B), or three (C–E) experiments performed, each of which gave similar results, is shown. *, $P < 0.05$; **, $P < 0.01$ (two-tailed Student's *t* test).

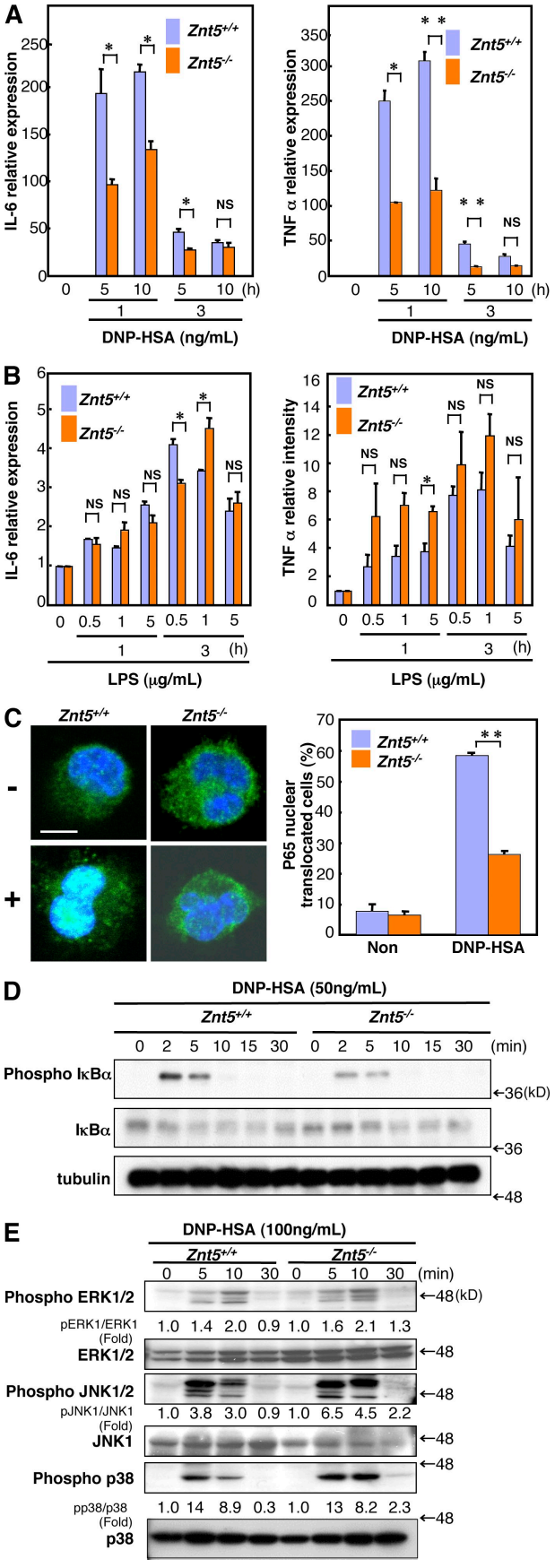

the C1 domain of PKC, the DAG-binding site. The C1 domain of PKC has two Zn finger–like motifs (Fig. 6 A) (39, 40). Based on the known function of the Zn finger, we hypothesized that the Zn finger–like motifs of PKC are required for translocation of PKC-β to the plasma membrane. To demonstrate this hypothesis, we designed WT–PKC-β–GFP and three mutant PKC-β–GFP constructs (Fig. 6 A) and examined their ability to undergo PMA-induced plasma membrane translocation in HeLa cells.

The WT and C1BS mutant form of PKC-β–GFP translocated equally well to the plasma membrane upon stimulation by PMA (Fig. 6 B and Videos 1 and 3). In contrast, the C1AS and C1ABS double mutant constructs did not translocate well and were retained in the cytoplasm (Fig. 6 B and Videos 2 and 4). These data suggested that the C1A Zn finger–like motif of PKC is important for its translocation to the plasma membrane and that this motif is a possible target for Znt5 and the likely binding site for DAG.

To test this hypothesis, we designed a biotin-conjugated PMA, an analogue of DAG (Biotinyl-PMA) (Fig. S10 A). Biotinyl-PMA induced cytokine production, just as PMA did (Fig. S10 B). Using Biotinyl-PMA, we assessed the binding ability of PMA to PKC-β. Transfected PKC-β WT and the C1AS mutant were extracted, run on a gel, and electrotransferred to a polyvinylidine fluoride (PVDF) membrane under native conditions. As shown in Fig. 6 C, Biotinyl-PMA expected to bind the PKC WT construct, but its signal intensity to the PKC C1AS mutant form was lower. Consistent with this result, the signal intensity of Biotinyl-PMA to PKC obtained from Znt5$^{-/-}$ BMMCs was less than that to PKC from WT BMMCs (Fig. 6 D).

Figure 4. Defective FcεRI-mediated NF-κB signaling in Znt5$^{-/-}$ BMMCs. Cells were sensitized with anti-DNP IgE and subsequently stimulated for 1 or 3 h with the indicated concentrations of DNP–HSA (A) or LPS (B). The mRNAs for IL-6 and TNF-α were measured by real-time quantitative RT-PCR. (A) FcεRI-induced IL-6 and TNF-α gene expression in Znt5$^{+/+}$ and Znt5$^{-/-}$ BMMCs. The expression level of nonstimulation was set as 1. Data show the mean + SD. (B) LPS-induced IL-6 and TNF-α gene expression in Znt5$^{+/+}$ and Znt5$^{-/-}$ BMMCs. Data show the mean + SD. (C, left) Confocal microscopy images of NF-κB nuclear translocation in cells stimulated with FcεRI (+) or not (−). Anti-p65 antibody staining (p65, green) and DAPI (nuclei, blue). Bar, 5 μm. (C, right) Frequency of cells with nuclear NF-κB. A Total of 50 cells were counted randomly in each experiment, and the frequency of NF-κB nuclear-translocated cells was calculated. Data show mean + SD. (D) IκBα phosphorylation and degradation were determined in Znt5$^{+/+}$ and Znt5$^{-/-}$ BMMCs stimulated with DNP-HSA for the indicated times. Cells were stimulated with FcεRI and immunoblotted with anti–phospho-IκBα, anti-IκBα, and tubulin. (E) FcεRI-induced MAPK activation in Znt5$^{+/+}$ and Znt5$^{-/-}$ BMMCs. The cell lysates were blotted with anti–phospho-ERK1/2, anti–phospho-JNK1/2, and anti–phospho-p38. The protein loading controls, which were used to normalize densitometric values, were anti-ERK1/2, anti-JNK1, and anti-p38, respectively. A representative dataset of the three (A, B, C, D [IκBα], and E) or four (D [phospho-IκBα]) experiments performed, each of which gave similar results, is shown. *, $P < 0.05$; **, $P < 0.01$ (two-tailed Student's *t* test).

DISCUSSION

Znt5 selectively regulates the mast cell–mediated delayed-type allergic response but not the immediate-type one

In this paper, we demonstrate that a Znt, Znt5, plays a crucial role in mast cell activation and mast cell–mediated allergic reactions. The mast cell is widely recognized as the most important effector cell in IgE-associated allergic disorders such as anaphylaxis. Previous experiments with genetically mast cell–deficient $Kit^{W}/Kit^{W\text{-}V}$ or $Kit^{W\text{-}sh}/Kit^{W\text{-}sh}$ mice have shown that mast cells are required for the IgE-mediated immediate-type

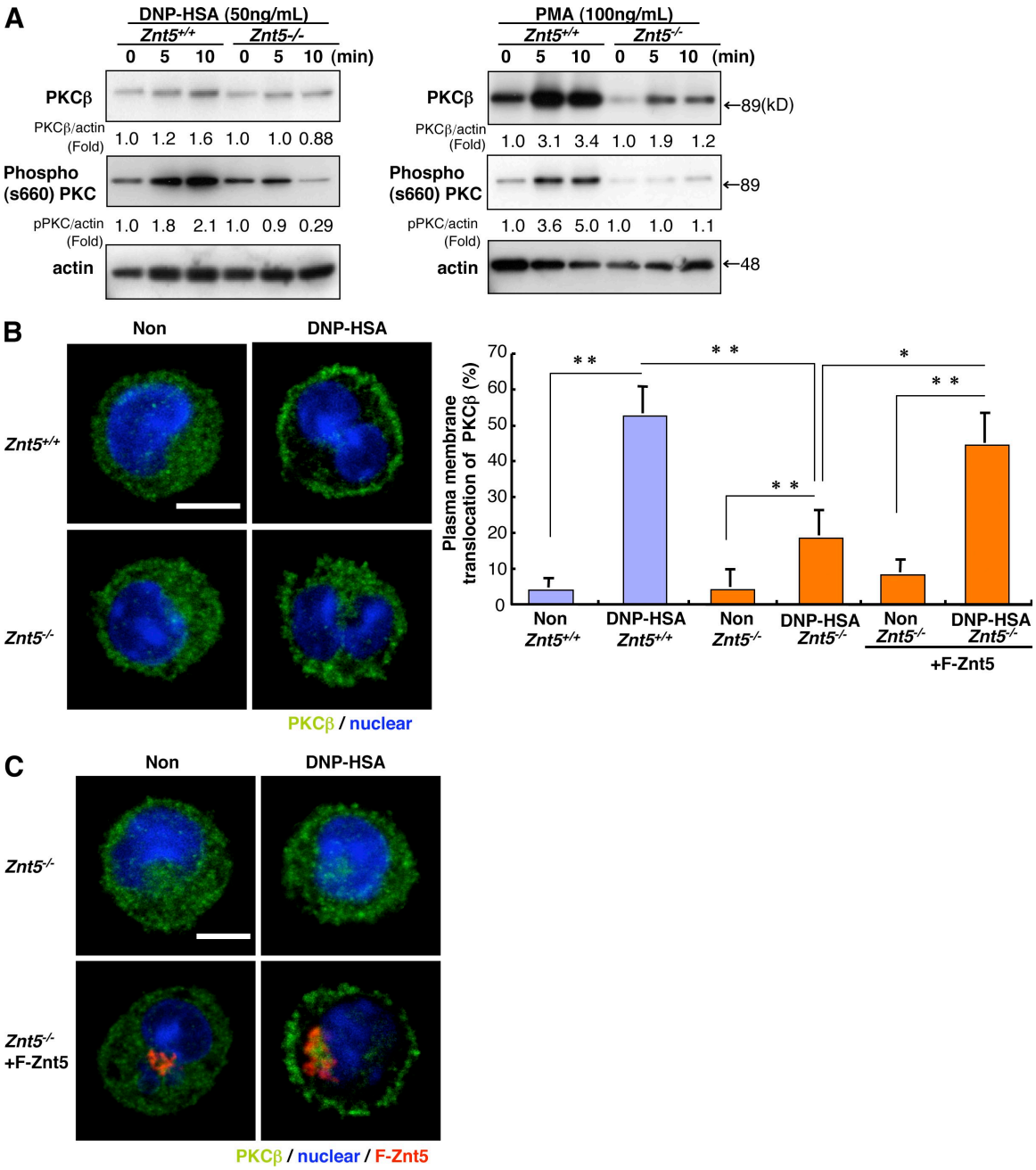

Figure 5. FcεRI or PMA-mediated plasma membrane translocation of PKC-β was impaired in $Znt5^{-/-}$ BMMCs. (A) FcεRI (left)- or PMA (right)-induced plasma membrane translocation of PKC in $Znt5^{+/+}$ and $Znt5^{-/-}$ BMMCs stimulated with DNP-HSA for the indicated times. The plasma membrane fraction was immunoblotted. The protein loading control, used to normalize densitometric values, was anti-actin. (B) PKC-β plasma membrane translocation observed by confocal microscopy. Cells were stimulated with DNP-HSA for 15 min or not (Non). Polyclonal anti-PKC-β antibody staining (green) and DAPI (blue) are shown. Bar, 5 µm. (C) Cells were double stained with anti-PKC-β antibody (green) and Zenon-conjugated anti-flag antibody (red). Nuclei were labeled with DAPI. Bar, 5 µm. The percentage of cells in the plasma membrane translocation of PKC-β is indicated on the right. 30 independent flag-Znt5–positive cells in $Znt5^{-/-}$ BMMCs were counted for each experiment. The values are the mean + SD. *, $P < 0.05$; **, $P < 0.01$, (two-tailed Student's *t* test). A representative dataset of the three (A and B) or five (C) experiments performed, each of which gave similar results, is shown.

allergic response (24, 27). Thus, the participation of mast cells in the immediate allergic reaction is well established. In addition to this classical role, much evidence has accumulated showing that mast cells play crucial roles in delayed-type allergic reactions and chronic inflammatory diseases, including arthritis, experimental allergic encephalomyelitis, colitis, and CHS (28, 52–54). A variety of mast cell–derived cytokines and chemokines are likely to be essential for delayed-type

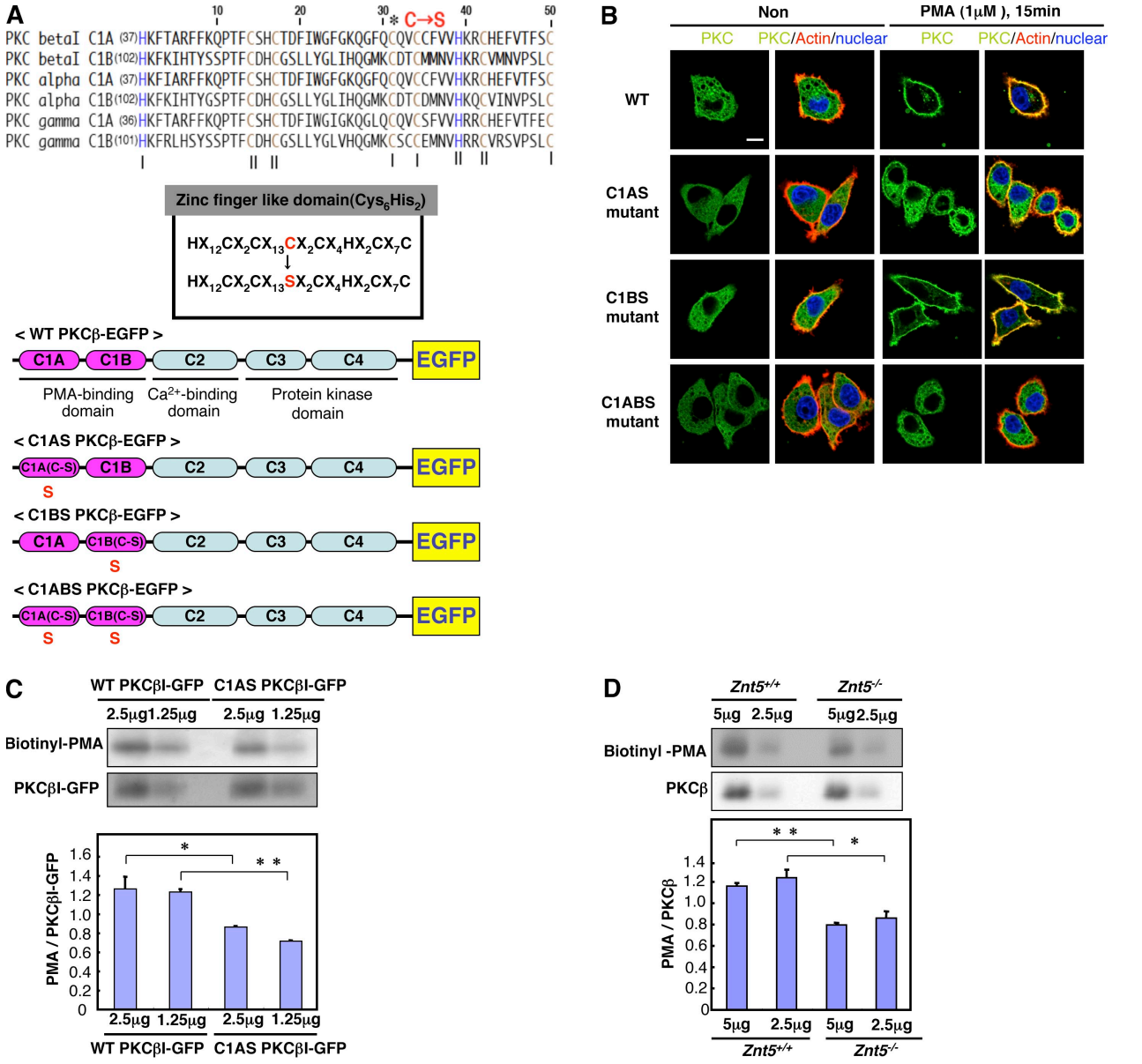

Figure 6. Zn finger–like motif of PKC is required for PMA-mediated translocation of PKC-β to the plasma membrane. (A, top) Alignment of C1 domains of conventional PKC family members. Brown, cysteine residues; blue, histidine residues. I and II indicate residues involved in the two Zn ion coordination sites. Asterisk indicates the position of the cysteine residue replaced by serine in this experiment. (A, bottom) Constructs for the PKC-β–GFP fusion protein and its mutants. WT PKC-β–EGFP carried the gene for EGFP at its C terminus. In the C1 region of PKC-β, there are two Zn finger–like sequences (top). To produce a Zn finger–like motif mutant form of PKC-β, one cysteine residue in each of the two cysteine-rich regions was replaced by serine by site-directed mutagenesis. (B) PMA-induced plasma membrane translocation of PKC-β observed by confocal microscopy. Localization of constructs in transfected HeLa cells stimulated with PMA or not (Non). F-actin and nuclei were labeled with phalloidin-rhodamine (red) and DAPI (blue), respectively. Bar, 10 μm. (C) PMA binding to PKC-β determined using biotinyl-PMA. 293T cells expressing WT–PKC-β–GFP and C1AS–PKC-β–GFP immunoblotted under native conditions (details in Materials and methods). The probes for PKC-β and biotinyl-PMA were anti-GFP antibody and streptavidin, respectively. (D) Cell lysates from Znt5$^{+/+}$ and Znt5$^{-/-}$ BMMCs resolved by native PAGE and blotted. (C and D) Densitometric values are shown below the blots. Data show mean + SD. *, $P < 0.05$; **, $P < 0.01$ (two-tailed Student's *t* test). A representative dataset of three (B–D) experiments performed, each of which gave similar results, is shown.

allergic reactions and chronic inflammatory diseases. In fact, the mast cell–defective $Kit^{W}/Kit^{W\text{-}V}$ mouse does not develop experimental allergic encephalomyelitis, and this defect is rescued by transferred WT BMMCs but not by IL-4–deficient BMMCs (55). These studies indicate that mast cell–derived cytokines are important in inflammatory diseases.

In this paper, we showed that $Znt5^{-/-}$ mast cells had an intact degranulation process but impaired cytokine and chemokine production. Most importantly, $Znt5^{-/-}$ mice had a defective mast cell–dependent delayed-type allergic reaction, i.e., CHS, but their immediate-type reaction, i.e., PCA, was unimpaired. Therefore, the $Znt5^{-/-}$ mouse will be valuable for further dissection of the in vivo roles of mast cells in immune and allergic responses and for analyzing the pathological status of a variety of immune-related diseases.

Znt5 is required for FcεRI-mediated NF-κB activation and the translocation of PKC to the plasma membrane

Our results showed that Znt5 is important for FcεRI-mediated cytokine or chemokine production. As Znt5 was mainly located in the Golgi, we first examined whether $Znt5^{-/-}$ mast cells were defective in cytokine processing/secretion. However, LPS-induced cytokine production was normal, indicating that the transport step was unaffected by the Znt5 deficiency in mast cells. We also observed that FcεRI induced normal activation of LAT and PLC-γ and calcium mobilization. This observation is consistent with our result showing normal degranulation in $Znt5^{-/-}$ BMMCs. From this, we deduced that the degranulation process can be induced in $Znt5^{-/-}$ mast cells as a result of intact calcium influx. Our results do not dispute the reported involvement of PKC in the degranulation process (35, 56), but this requirement for PKC may be compensated by other signaling pathways in $Znt5^{-/-}$ mast cells. Alternatively, the threshold of the degree of PKC activation required for degranulation and that for NF-κB activation might be different. To support this idea, we performed PKC family inhibitor experiment and showed that PKC inhibitor-treated $Znt5^{-/-}$ mast cells were significantly reduced by FcεRI-mediated degranulation (Fig. S11).

We found that FcεRI-mediated NF-κB activation was defective in the $Znt5^{-/-}$ BMMCs; FcεRI-induced nuclear translocation of p65 was reduced, and FcεRI-mediated IκBα phosphorylation and its subsequent degradation were impaired. From these results, we concluded that Znt5 is selectively required for FcεRI-mediated NF-κB activation but not for MAPK activation or calcium mobilization. Because the expression of IL-6 and TNF-α depend on the activation of NF-κB, which is a master transcription factor that regulates the expression of proinflammatory cytokine and chemokine genes (57), our results indicated that Znt5 is a novel player involved in FcεRI-induced cytokine production through NF-κB activation.

PKC-θ and PKC-β play important roles in NF-κB activation and function upstream of the Bcl10–MALT1 complex in TCR and BCR signaling (41, 42). In mast cells, PKC is responsible for the activation of NF-κB; for example, a PKC inhibitor suppresses NF-κB activation (23, 51). Furthermore, PKC-β–deficient mast cells are defective in IL-6 production (58). In this paper, we showed that Znt5 was required for the FcεRI- or PMA-induced translocation of PKC-β to the plasma membrane of BMMCs, and this requirement explains why Znt5 is needed for NF-κB activation.

A related question is how Znt5 regulates the plasma membrane translocation of PKC-β, and several of our findings relate to this issue: the C1A Zn finger–like motif of PKC-β was required for translocation of PKC to the plasma membrane; mutating the C1A Zn finger–like motif of PKC-β diminished its ability to bind PMA; PKC obtained from $Znt5^{-/-}$ BMMCs showed decreased binding to PMA; Znt5 was located in the Golgi; and $Znt5^{-/-}$ BMMCs showed an increase in cytoplasmic free Zn. Because Znt5 was located in the Golgi, it probably promotes a Zn efflux from the cytoplasm into the Golgi. Because $Znt5^{-/-}$ BMMCs had increased cytoplasmic free Zn, it seems likely that the available Zn in the Golgi was decreased concomitantly.

Together, these observations suggested the hypothesis that in the $Znt5^{-/-}$ BMMCs, the Zn available to the C1A Zn finger–like motif of PKC as it transits through the Golgi is decreased, which results in an increase in Zn-free PKC. The mutation of the Zn-binding site of C1A interfered with the plasma membrane translocation of PKC, and this mutation also diminished PMA binding to PKC. Collectively, our findings suggest that binding of Zn to the C1A of PKC induces a conformational change required for DAG binding, which is itself required for the translocation of PKC to the plasma membrane. This hypothesis is supported by our data as well as by findings from other groups that Zn is involved in the translocation of PKC to the plasma membrane (59–61). Furthermore, in experiments using $Znt5^{-/-}$ DT40 cells, Suzuki et al. (48, 62) showed that Znt5 expressed on the ER-Golgi membrane is required for the enzymatic activity of the Zn-dependent alkaline phosphatases (ALPs), which are processed from apoALPs to holoALPs in the ER-Golgi.

In summary, the results in this paper show that a Znt, Znt5, is selectively required for the mast cell–mediated delayed-type allergic response but not for the immediate-type allergic reaction. We further showed that Znt5 is required in the PKC-mediated NF-κB signaling pathway. The identification of Znt5 as a novel component of FcεRI-mediated PKC activation sheds light on the molecular mechanisms of the processing and activation of PKC and of the Zn-mediated regulation of mast cell–dependent allergic responses, specifically of the delayed type.

MATERIALS AND METHODS

Mice. C57BL/6J mice were obtained from CREA Japan. $Znt5^{-/-}$ mice were provided by Y. Nakamura and T. Tanaka (University of Tokyo, Tokyo, Japan, and RIKEN, Center for Genomic Medicine, Kanagawa, Japan). The generation of $Znt5^{-/-}$ mouse was reported in detail by Inoue et al. (44). Mast cell–deficient $Kit^{W\text{-}sh/W\text{-}sh}$ mice were provided by the RIKEN BioResource Center. We obtained approval from the Animal Research Committee at RIKEN for all animal experiments performed.

Antibodies and reagents. Anti-Znt5 antibodies were raised by immunizing rabbits with KLH-conjugated peptide (TIQVEKEAYFQHMSG). For the immunization, rabbits were first injected with 200 μg of KLH-conjugated Znt5 peptide in complete Freund's adjuvant and then boosted every week with 50 μg of the antigen in incomplete Freund's adjuvant. Anti-GFP and antiphosphotyrosine (4G10) antibodies were purchased from MBL and Millipore, respectively. Anti-Flag (M2), anti-GM130, anti–PKC-β (C-16), anti–phospho-PKC (S660), and anti-LAT antibodies were obtained from Sigma-Aldrich, BD, Santa Cruz Biotechnology, Inc., Cell Signaling Technology, and Millipore, respectively. Gö6976 was purchased from EMD.

FITC-induced CHS. The FITC-induced CHS procedure was performed as described previously (31). In brief, mice were sensitized with a total of 200 μl of 2% FITC isomer-I (FITC; Sigma-Aldrich) in a vehicle consisting of acetone-dibutylphthalate (1:1) applied to the skin of the back. 5 d after the sensitization with FITC, the mice were challenged with 40 μl of vehicle alone on the right ear (20 μl on each side of the ear) and 0.5% FITC on the left ear (20 μl on each side). Ear thickness was measured before and at multiple intervals after FITC challenge with an engineer's microcaliper (Ozaki). Some mice from each group were killed 24 h after the FITC or vehicle challenge for cytokine analysis.

For mast cell reconstitution studies, BMMCs were injected intradermally (1.0×10^6 cells in 20 μl/ear for CHS) in 6-wk-old $Kit^{W\text{-}sh/W\text{-}sh}$ mice. The mice were used for CHS experiments at 6 wk after transfer of BMMCs.

PCA and histology of the ears. A total of 2 μg IgE was injected subcutaneously into ears for 12 h. After this sensitization, the mice were then challenged with an intravenous injection of 250 μg of polyvalent DNP-BSA (Cosmo Bio Co., LTD.) in 250 μl of saline and 5 mg/ml of Evans blue dye (Sigma-Aldrich). The extravasation of Evans blue into the ear was monitored for 30 min. The mice were then sacrificed, both ears were dissected, and the Evans blue dye was extracted in 700 μl of formamide at 63°C overnight. The absorbance of the Evans blue–containing formamide was then measured at 620 nm. To observe the ear mast cells, 3-μm paraffin sections were fixed and stained with nuclear fast red and Alcian blue, and the Alcian blue–stained cells in each sample were counted. All data are expressed as the number of mast cells per mm^2 of dermis.

Primary mast cell cultures and cell lines. BMMCs were prepared as described previously (63). In brief, BM cells were flushed from the marrow cavity of mouse femurs, and the mast cells (BMMCs) were selectively grown in RPMI1640 medium supplemented with IL-3 (conditioned medium from an mIL-3–producing cell line, CHOmIL-3-3-12M [gift from T. Sudo, Toray Industries, Inc., Kamakura, Japan]), 10% FBS, 10 mU/ml penicillin, and 0.1 mg/ml streptomycin for 4–8 wk. During culture, the medium was changed every 3–4 d, and the cells were transferred to new dishes to eliminate adherent cells. After 5 wk in culture, the BMMCs were ready for in vitro experiments and showed the cell surface expression of FcεRI and c-Kit. HeLa cells were maintained in RPMI1640 supplemented with 10% FBS, penicillin, and streptomycin.

Degranulation assay. The degranulation assay was described previously (64). In brief, the degree of degranulation was determined by measuring the release of β-hexosaminidase. 1×10^6 cells/ml were preloaded with 1 μg/ml anti-DNP IgE (SPE-7; Sigma-Aldrich) by a 6-h incubation in medium (without IL-3). To measure β-hexosaminidase release, the sensitized cells were stimulated with 100 ng/ml DNP-HSA for 30 min in Tyrode's buffer. Samples were placed on ice and then spun at 4°C for 5 min. The enzymatic activities of β-hexosaminidase in the supernatants and cell pellets solubilized with 1% Triton X-100 in Tyrode's buffer were measured with *p*-nitrophenyl *N*-acetyl-β-D-glucosaminide (Sigma-Aldrich) in 0.1 M sodium citrate, pH 4.5, for 60 min at 37°C. The reaction was stopped by the addition of 0.2 M glycine, pH 10.7. The release of the product 4-*p*-nitrophenol was detected by absorbance at 405 nm. The extent of degranulation was calculated by dividing the 4-*p*-nitrophenol absorbance in the supernatant by the sum of the absorbance in the supernatant and detergent-solubilized cell pellet.

Measurement of cytokines and chemical mediators. Cells were activated as described in the previous sections, and TNF-α and IL-6 in the cell culture supernatants were measured with an ELISA kit (eBioscience). The leukotrienes were quantified using an ELISA kit (Cayman Chemical), according to the manufacturer's instructions.

Cell lysates and immunoblotting. 1×10^6/ml BMMCs were sensitized with 1 μg/ml IgE for 6 h at 37°C. Cells were stimulated with 100 ng/ml DNP-HSA. After the stimulation, the cells were harvested and lysed with 100 μl of lysis buffer (20 mM Tris-HCl, pH 7.4, at 4°C, 150 mM NaCl, 1% NP-40, 0.1% SDS, 0.1% deoxycholate, 1 mM $NaVO_4$, 3 mM EDTA, and proteinase inhibitors [0.5 mM PMSF, 10 μg/ml aprotinin, 5 μg/ml pepstatin, and10 μg/ml leupeptin]) for 30 min at 4°C and spun at 15,000 *g* at 4°C for 15 min. The eluted and reduced samples were resolved by SDS-PAGE using a 5–20% gradient polyacrylamide gel (Wako Chemicals USA, Inc.) and transferred to a PVDF membrane (Immobilon-P; Millipore). For immunoblotting, the membranes were incubated with anti–phospho-ERK, anti–phospho-JNK, anti–phospho-p38, anti-ERK, anti-JNK, anti-p38, anti–phospho-IκBα, anti-IκBα, anti–β-tubulin, anti-actin, and anti–PKC-β, respectively. For immunoprecipitation, the cell lysates were incubated for 4 h at 4°C with 1 μg of antibodies bound to protein A Sepharose. The eluted and reduced samples were separated on a 5–20% gradient SDS-polyacrylamide gel and transferred to a PVDF membrane. The membranes were incubated with antiphosphotyrosine. After blotting with the first antibody, the membranes were blotted with HRP-conjugated species-specific anti-IgG (Invitrogen) for 1 h at room temperature. After extensive washing of the membranes, the immunoreactive proteins were visualized using the Renaissance chemiluminescence system (Dupont), according to the manufacturer's recommendations. The PVDF membranes were exposed to RX film (Fujifilm). Densitometric analysis for tubulin and PKC-β was performed using a fluorescence image analyzer (LAS-1000; Fujifilm).

Preparation of plasma membrane protein. Plasma membrane proteins were extracted using a Plasma Membrane Protein Extraction kit (K268-50; BioVision, Inc.), according to the manufacturer's instructions. The plasma membrane fractions were used for immunoblotting and probed with anti-actin, anti–PKC-β, and anti–phospho-PKC (S660). Densitometric analysis for PKC-β, phospho-PKC (S660), and actin was performed using an LAS-1000 fluorescence image analyzer.

Confocal microscopy. Separate aliquots of 5×10^5 cells were sensitized with 1 μg/ml IgE for 6 h. The cells were then stimulated with 100 ng/ml DNP-HSA for 10 min at 37°C and fixed with 4% paraformaldehyde for 30 min. The cells were spun and permeabilized in Perm Buffer (BD) containing 1% BSA for 15 min at room temperature. The cells were washed with 1 ml PBS^- (PBS without calcium and magnesium) twice, resuspended in 500 μl of PBS^-, and attached to glass slides by cytospin (Thermo Fisher Scientific) for 5 min. Primary and secondary staining were performed on the slides, with anti-p65 at a dilution of 1:50, anti–PKC-β at 1:100, Alexa Fluor 488–conjugated anti–rabbit IgG (Invitrogen) at 1:100, and phalloidin-rhodamine (Invitrogen) at 1:100. Confocal microscopy was performed using the TCS SL system (Leica).

RT-PCR and real-time quantitative RT-PCR analysis. Cells were homogenized with Sepasol RNAI (Nacalai Tesque, Inc.), and the total RNA was isolated according to the manufacturer's instructions. For standard RT-PCR, cDNA was synthesized from 500 ng of total RNA by RT (ReverTra Ace; TOYOBO) and 500 ng of oligo (dT) primer (Invitrogen) for 30 min at 42°C. A portion of the cDNA (typically 1/20 vol) was used for standard PCR to detect IL-6, TNF-α, and GAPDH. 25 cycles of PCR were performed with 0.5 U rTaq DNA polymerase and 10 pmol of gene-specific sense and antisense primers. For real-time quantitative RT-PCR, IL-6 and TNF-α gene expression was measured relative to

GAPDH using the SYBR Green system (Applied Biosystems). Primers used in these experiments were purchased from Invitrogen, and the sequences were as follows: IL-6 forward, 5′-GAGGATACCACTCCCAACAGACC-3′ and reverse, 5′-AAGTGCATCATCGTTGTTCATACA-3′; TNF-α forward, 5′-CATCTTCTCAAAATTCGAGTGACAA-3′ and reverse, 5′-TGGGAGTAGACAAGGTACAACCC-3′; GAPDH forward, 5′-TTCACCACCATGGAGAAGGCCG-3′ and reverse, 5′-GGCATGGACTGTGGTCATGA-3′; and hypoxanthine-guanine phosphoribosyl transferase forward, 5′-CCTCCCATCTCCTTCATGACA-3′ and reverse, 5′-GATTAGCGATGATGAACCAGGTT-3′. In addition, primers used for amplifying cDNAs for Znt family members and other primer sets are listed in Table S1. PCR products were separated on an agarose gel, stained with 500 ng/ml ethidium bromide, and photographed.

Intracellular Zn measurement. 2×10^6 BMMCs were treated with 2.5 μM of Newport green for 30 min at 37°C. The cells were washed two times with PBS^- before the fluorescence intensity was measured by FACS. The concentration of intracellular free Zn was calculated from the mean fluorescence with the formula $[Zn] = K_D \times [(F - F_{min})/(F_{max} - F)]$. The dissociation constant of the Newport Green/Zn complex is 1 μM. F_{min} was determined by the addition of the Zn-specific membrane-permeant chelator TPEN, and F_{max} was determined by the addition of $ZnSO_4$ and the ionophore pyrithione (65).

Calcium influx measurement. 1×10^6 BMMCs/ml were sensitized with 1 μg/ml IgE (anti-DNP IgE clone SPE-7; Sigma-Aldrich) for 6 h at 37°C. IgE-sensitized mast cells were washed three times, resuspended in Tyrode's buffer (10 mM Hepes, pH 7.4, 130 mM NaCl, 5 mM KCl, 1.4 mM $CaCl_2$, 1 mM $MgCl_2$, and 5.6 mM glucose), allowed to adhere to a poly-L-lysine–coated glass-bottom dish, and incubated with 5 μM Fluo-4, a cell-permeant dye, for 30 min at 37°C. Surplus fluorescence indicator and floating cells were removed by at least three washes with Tyrode's buffer. Cells were stimulated with 100 ng/ml DNP–HSA (Sigma-Aldrich) at 37°C. Images of the fluorescent signals were captured every 10 or 30 s from an inverted microscope (Axiovert 200 MOT; Carl Zeiss, Inc.) equipped with an oil Plan Neofluar 100× 1.3 NA objective, a charge-coupled device camera (Cool Snap HQ; Roper Scientific), and the system control application SlideBook (Intelligent Imaging Innovation) at 25°C. The captured images were processed with Photoshop software (Adobe) to adjust their size and contrast.

cDNA cloning and plasmid construction. PKC-β was cloned by PCR using cDNA from BMMCs and sequenced on a 3130xl sequencer (ABI-PRISM; APplied Biosystems). The GFP-tagged expression vectors for PKC-β were constructed and subcloned into pEGFP N1 (Invitrogen). The construct encoding mutant PKC-β–GFP, in which the Zn finger–like motif in the C1 region was mutated, was made using a PCR-based method. The human Znt5 cDNA in pA-Zeocin was reported in detail by Suzuki et al. (62). HeLa cells were transfected with a total of 1 μg PKC-β cDNA in pEGFP or with empty vector using Lipofectamine 2000 (Invitrogen).

Retroviral infection. Retroviral infection was performed as previously described (64). The Flag-tagged human Znt5 plasmid (gift from T. Kambe and T. Suzuki, Kyoto University, Kyoto, Japan) was inserted into the BamHI and NotI sites of the retroviral vector pMX (gift from T. Kitamura, University of Tokyo, Tokyo, Japan). This construct was then used to transfect the 293T-based packaging cell line phoenix (gift from G. Nolan, Stanford University, Stanford, CA), with Lipofectamine 2000 (Invitrogen) to generate recombinant retroviruses. BM cells were infected with the retrovirus in the presence of 10 μg/ml polybrene (Sigma-Aldrich) and IL-3.

Biotinyl-PMA and native PAGE. PMA (Nacalai Tesque, Inc.) was conjugated with biotin (Wako Chemicals USA, Inc.). The predicted biotinyl-PMA is shown in Fig. S10. Native PAGE was performed with the NativePAGE Novex Bis-Tris Gel system (Invitrogen). In detail, the cells were lysed with NativePAGE Sample buffer for 10 min at 4°C and spun at 15,000 *g* at 4°C for 10 min. The samples were separated by native PAGE on 4–16% Bis-Tris Gels and transferred to a PVDF membrane (Immobilon-P; Millipore). For immunoblotting, the membrane was incubated with Biotinyl-PMA or anti–PKC-β antibody. After the membrane was washed in TBST, the coloring reaction was performed with streptavidin-AP (Roche) or anti–rabbit IgG HRP antibody, respectively. Densitometric analysis for PKC-β and PMA was performed using an LAS-1000 fluorescence image analyzer (Fujifilm).

Statistical analysis. All data were analyzed with Statcell (Microsoft). Data were considered statistically significant for p-values <0.05, obtained with a two-tailed Student's *t* test.

Online supplemental material. Fig. S1 shows expression level of Znt family member in BMMCs. Fig. S2 shows expression level of Znt5 after antigen stimulation. Fig. S3 shows normal development of BMMC from $Znt5^{-/-}$ mice. Fig. S4 shows normal development of mast cell in $Znt5^{-/-}$ mice. Fig. S5 shows numbers of mast cells in dermis from vehicle-treated or FITC-challenged ears. Fig. S6 shows quantitative analysis of IκBα phosphorylation and degradation. Fig. S7 shows normal FcεRI-induced calcium signaling and influx in $Znt5^{-/-}$ BMMCs. Fig. S8 shows impairment of PKC activity in $Znt5^{-/-}$ BMMCs. Fig. S9 shows normal expression levels of PKC-β in $Znt5^{-/-}$ BMMCs. Fig. S10 shows design of biotinyl-PMA and that biotinyl-PMA can induce cytokine production. Fig. S11 shows that the PKC inhibitor Gö6976 inhibits FcεRI-induced degranulation in $Znt5^{-/-}$ BMMCs. Video 1 shows time-lapse images of WT PKC-β–EGFP in HeLa cells after PMA stimulation. Video 2 shows time-lapse images of C1AS PKC-β–EGFP in HeLa cells after PMA stimulation. Video 3 shows time-lapse images of C1BS PKC-β–EGFP in HeLa cells after PMA stimulation. Video 4 shows time-lapse images of C1ABS PKC-β–EGFP in HeLa cells after PMA stimulation. Online supplemental material is available at http://www.jem.org/cgi/content/full/jem.20082533/DC1.

We thank Drs. Y. Nakamura and T. Tanaka (University of Tokyo and RIKEN, Center for Genomic Medicine) for providing the $Znt5^{-/-}$ mice. We would like to thank Drs. P. Burrows for critical readings and K. Kabu, T. Suzuki, T. Kambe, A. Hijikata, H. Shinohara, H. Kitamura, and H. Watarai for technical advice and suggestions. We also thank Ms. A. Ito, Ms. M. Yamada, Ms. M. Hara, Mr. S. Fukuda, and Ms. N. Hashimoto for excellent technical assistance and Ms. M. Shimura for secretarial assistance.

This work was supported by grants from the Ministry of Education, Culture, Sports, Science and Technology in Japan.

The authors have no conflicting financial interests.

Submitted: 7 November 2008
Accepted: 22 April 2009

REFERENCES

1. Vallee, B.L., and K.H. Falchuk. 1993. The biochemical basis of zinc physiology. *Physiol. Rev.* 73:79–118.
2. Prasad, A.S. 1995. Zinc: an overview. *Nutrition.* 11:93–99.
3. Rink, L., and P. Gabriel. 2000. Zinc and the immune system. *Proc. Nutr. Soc.* 59:541–552.
4. Fernandes, G., M. Nair, K. Onoe, T. Tanaka, R. Floyd, and R.A. Good. 1979. Impairment of cell-mediated immunity functions by dietary zinc deficiency in mice. *Proc. Natl. Acad. Sci. USA.* 76:457–461.
5. Fraker, P.J., R. Caruso, and F. Kierszenbaum. 1982. Alteration of the immune and nutritional status of mice by synergy between zinc deficiency and infection with *Trypanosoma cruzi*. *J. Nutr.* 112:1224–1229.
6. Keen, C.L., and M.E. Gershwin. 1990. Zinc deficiency and immune function. *Annu. Rev. Nutr.* 10:415–431.
7. Ibs, K.H., and L. Rink. 2003. Zinc-altered immune function. *J. Nutr.* 133:1452S–1456S.
8. Eide, D.J. 2004. The SLC39 family of metal ion transporters. *Pflugers Arch.* 447:796–800.
9. Vallee, B.L., and D.S. Auld. 1995. Zinc metallochemistry in biochemistry. *EXS.* 73:259–277.
10. Andrews, G.K. 2001. Cellular zinc sensors: MTF-1 regulation of gene expression. *Biometals.* 14:223–237.

11. Palmiter, R.D., and L. Huang. 2004. Efflux and compartmentalization of zinc by members of the SLC30 family of solute carriers. *Pflugers Arch.* 447:744–751.
12. Kambe, T., Y. Yamaguchi-Iwai, R. Sasaki, and M. Nagao. 2004. Overview of mammalian zinc transporters. *Cell. Mol. Life Sci.* 61:49–68.
13. Eide, D.J. 2006. Zinc transporters and the cellular trafficking of zinc. *Biochim. Biophys. Acta.* 1763:711–722.
14. Williams, R.J. 1984. Zinc: what is its role in biology? *Endeavour.* 8:65–70.
15. Grummt, F., C. Weinmann-Dorsch, J. Schneider-Schaulies, and A. Lux. 1986. Zinc as a second messenger of mitogenic induction. Effects on diadenosine tetraphosphate (Ap4A) and DNA synthesis. *Exp. Cell Res.* 163:191–200.
16. Csermely, P., and J. Somogyi. 1989. Zinc as a possible mediator of signal transduction in T lymphocytes. *Acta Physiol. Hung.* 74:195–199.
17. Hirano, T., M. Murakami, T. Fukada, K. Nishida, S. Yamasaki, and T. Suzuki. 2008. Roles of zinc and zinc signaling in immunity: zinc as an intracellular signaling molecule. *Adv. Immunol.* 97:149–176.
18. Bruinsma, J.J., T. Jirakulaporn, A.J. Muslin, and K. Kornfeld. 2002. Zinc ions and cation diffusion facilitator proteins regulate Ras-mediated signaling. *Dev. Cell.* 2:567–578.
19. Taylor, K.M., P. Vichova, N. Jordan, S. Hiscox, R. Hendley, and R.I. Nicholson. 2008. ZIP7-mediated intracellular zinc transport contributes to aberrant growth factor signaling in antihormone-resistant breast cancer Cells. *Endocrinology.* 149:4912–4920.
20. Yamashita, S., C. Miyagi, T. Fukada, N. Kagara, Y.S. Che, and T. Hirano. 2004. Zinc transporter LIVI controls epithelial-mesenchymal transition in zebrafish gastrula organizer. *Nature.* 429:298–302.
21. Kitamura, H., H. Morikawa, H. Kamon, M. Iguchi, S. Hojyo, T. Fukada, S. Yamashita, T. Kaisho, S. Akira, M. Murakami, and T. Hirano. 2006. Toll-like receptor-mediated regulation of zinc homeostasis influences dendritic cell function. *Nat. Immunol.* 7:971–977.
22. Yamasaki, S., K. Sakata-Sogawa, A. Hasegawa, T. Suzuki, K. Kabu, E. Sato, T. Kurosaki, S. Yamashita, M. Tokunaga, K. Nishida, and T. Hirano. 2007. Zinc is a novel intracellular second messenger. *J. Cell Biol.* 177:637–645.
23. Kabu, K., S. Yamasaki, D. Kamimura, Y. Ito, A. Hasegawa, E. Sato, H. Kitamura, K. Nishida, and T. Hirano. 2006. Zinc is required for FcepsilonRI-mediated mast cell activation. *J. Immunol.* 177:1296–1305.
24. Miyajima, I., D. Dombrowicz, T.R. Martin, J.V. Ravetch, J.P. Kinet, and S.J. Galli. 1997. Systemic anaphylaxis in the mouse can be mediated largely through IgG1 and Fc gammaRIII. Assessment of the cardiopulmonary changes, mast cell degranulation, and death associated with active or IgE- or IgG1-dependent passive anaphylaxis. *J. Clin. Invest.* 99:901–914.
25. Galli, S.J. 1993. New concepts about the mast cell. *N. Engl. J. Med.* 328:257–265.
26. Galli, S.J., J. Kalesnikoff, M.A. Grimbaldeston, A.M. Piliponsky, C.M. Williams, and M. Tsai. 2005. Mast cells as "tunable" effector and immunoregulatory cells: recent advances. *Annu. Rev. Immunol.* 23:749–786.
27. Wershil, B.K., Y.A. Mekori, T. Murakami, and S.J. Galli. 1987. 125I-fibrin deposition in IgE-dependent immediate hypersensitivity reactions in mouse skin. Demonstration of the role of mast cells using genetically mast cell-deficient mice locally reconstituted with cultured mast cells. *J. Immunol.* 139:2605–2614.
28. Wershil, B.K., Z.S. Wang, J.R. Gordon, and S.J. Galli. 1991. Recruitment of neutrophils during IgE-dependent cutaneous late phase reactions in the mouse is mast cell-dependent. Partial inhibition of the reaction with antiserum against tumor necrosis factor-alpha. *J. Clin. Invest.* 87:446–453.
29. Grabbe, S., and T. Schwarz. 1996. Immunoregulatory mechanisms involved in elicitation of allergic contact hypersensitivity. *Am. J. Contact Dermat.* 7:238–246.
30. Biedermann, T., M. Kneilling, R. Mailhammer, K. Maier, C.A. Sander, G. Kollias, S.L. Kunkel, L. Hultner, and M. Rocken. 2000. Mast cells control neutrophil recruitment during T cell–mediated delayed-type hypersensitivity reactions through tumor necrosis factor and macrophage inflammatory protein 2. *J. Exp. Med.* 192:1441–1452.
31. Suto, H., S. Nakae, M. Kakurai, J.D. Sedgwick, M. Tsai, and S.J. Galli. 2006. Mast cell-associated TNF promotes dendritic cell migration. *J. Immunol.* 176:4102–4112.
32. Gordon, J.R., P.R. Burd, and S.J. Galli. 1990. Mast cells as a source of multifunctional cytokines. *Immunol. Today.* 11:458–464.
33. Gordon, J.R., and S.J. Galli. 1990. Mast cells as a source of both preformed and immunologically inducible TNF-alpha/cachectin. *Nature.* 346:274–276.
34. Baumgartner, R.A., K. Yamada, V.A. Deramo, and M.A. Beaven. 1994. Secretion of TNF from a rat mast cell line is a brefeldin A-sensitive and a calcium/protein kinase C-regulated process. *J. Immunol.* 153:2609–2617.
35. Chang, E.Y., Z. Szallasi, P. Acs, V. Raizada, P.C. Wolfe, C. Fewtrell, P.M. Blumberg, and J. Rivera. 1997. Functional effects of overexpression of protein kinase C-alpha, -beta, -delta, -epsilon, and -eta in the mast cell line RBL-2H3. *J. Immunol.* 159:2624–2632.
36. Csermely, P., M. Szamel, K. Resch, and J. Somogyi. 1988. Zinc can increase the activity of protein kinase C and contributes to its binding to plasma membranes in T lymphocytes. *J. Biol. Chem.* 263:6487–6490.
37. Csermely, P., M. Szamel, K. Resch, and J. Somogyi. 1988. Zinc increases the affinity of phorbol ester receptor in T lymphocytes. *Biochem. Biophys. Res. Commun.* 154:578–583.
38. Forbes, I.J., P.D. Zalewski, C. Giannakis, H.S. Petkoff, and P.A. Cowled. 1990. Interaction between protein kinase C and regulatory ligand is enhanced by a chelatable pool of cellular zinc. *Biochim. Biophys. Acta.* 1053:113–117.
39. Sakai, N., K. Sasaki, N. Ikegaki, Y. Shirai, Y. Ono, and N. Saito. 1997. Direct visualization of the translocation of the γ-subspecies of protein kinase C in living cells using fusion proteins with green fluorescent protein. *J. Cell Biol.* 139:1465–1476.
40. Corbalan-Garcia, S., and J.C. Gomez-Fernandez. 2006. Protein kinase C regulatory domains: the art of decoding many different signals in membranes. *Biochim. Biophys. Acta.* 1761:633–654.
41. Sun, Z., C.W. Arendt, W. Ellmeier, E.M. Schaeffer, M.J. Sunshine, L. Gandhi, J. Annes, D. Petrzilka, A. Kupfer, P.L. Schwartzberg, and D.R. Littman. 2000. PKC-theta is required for TCR-induced NF-kappaB activation in mature but not immature T lymphocytes. *Nature.* 404:402–407.
42. Su, T.T., B. Guo, Y. Kawakami, K. Sommer, K. Chae, L.A. Humphries, R.M. Kato, S. Kang, L. Patrone, R. Wall, et al. 2002. PKC-beta controls I kappa B kinase lipid raft recruitment and activation in response to BCR signaling. *Nat. Immunol.* 3:780–786.
43. Klemm, S., J. Gutermuth, L. Hultner, T. Sparwasser, H. Behrendt, C. Peschel, T.W. Mak, T. Jakob, and J. Ruland. 2006. The Bcl10–Malt1 complex segregates FcεRI-mediated nuclear factor κB activation and cytokine production from mast cell degranulation. *J. Exp. Med.* 203:337–347.
44. Inoue, K., K. Matsuda, M. Itoh, H. Kawaguchi, H. Tomoike, T. Aoyagi, R. Nagai, M. Hori, Y. Nakamura, and T. Tanaka. 2002. Osteopenia and male-specific sudden cardiac death in mice lacking a zinc transporter gene, Znt5. *Hum. Mol. Genet.* 11:1775–1784.
45. Kambe, T., T. Suzuki, M. Nagao, and Y. Yamaguchi-Iwai. 2006. Sequence similarity and functional relationship among eukaryotic ZIP and CDF transporters. *Genomics Proteomics Bioinformatics.* 4:1–9.
46. Hijikata, A., H. Kitamura, Y. Kimura, R. Yokoyama, Y. Aiba, Y. Bao, S. Fujita, K. Hase, S. Hori, Y. Ishii, O. Kanagawa, H. Kawamoto, K. Kawano, H. Koseki, M. Kubo, A. Kurita-Miki, T. Kurosaki, K. Masuda, M. Nakata, K. Oboki, H. Ohno, M. Okamoto, Y. Okayama, J. O-Wang, H. Saito, T. Saito, M. Sakuma, K. Sato, K. Sato, K. Seino, R. Setoguchi, Y. Tamura, M. Tanaka, M. Taniguchi, I. Taniuchi, A. Teng, T. Watanabe, H. Watarai, S. Yamasaki, and O. Ohara. 2007. Construction of an open-access database that integrates cross-reference information from the transcriptome and proteome of immune cells. *Bioinformatics.* 23:2934–2941.
47. Kambe, T., H. Narita, Y. Yamaguchi-Iwai, J. Hirose, T. Amano, N. Sugiura, R. Sasaki, K. Mori, T. Iwanaga, and M. Nagao. 2002. Cloning and characterization of a novel mammalian zinc transporter, zinc transporter 5, abundantly expressed in pancreatic beta cells. *J. Biol. Chem.* 277:19049–19055.

48. Suzuki, T., K. Ishihara, H. Migaki, W. Matsuura, A. Kohda, K. Okumura, M. Nagao, Y. Yamaguchi-Iwai, and T. Kambe. 2005. Zinc transporters, ZnT5 and ZnT7, are required for the activation of alkaline phosphatases, zinc-requiring enzymes that are glycosylphosphatidylinositol-anchored to the cytoplasmic membrane. *J. Biol. Chem.* 280:637–643.
49. Wang, B., C. Esche, A. Mamelak, I. Freed, H. Watanabe, and D.N. Sauder. 2003. Cytokine knockouts in contact hypersensitivity research. *Cytokine Growth Factor Rev.* 14:381–389.
50. Rivera, J. 2002. Molecular adapters in Fc(epsilon)RI signaling and the allergic response. *Curr. Opin. Immunol.* 14:688–693.
51. Peng, Y., M.R. Power, B. Li, and T.J. Lin. 2005. Inhibition of IKK down-regulates antigen + IgE-induced TNF production by mast cells: a role for the IKK-IkappaB-NF-kappaB pathway in IgE-dependent mast cell activation. *J. Leukoc. Biol.* 77:975–983.
52. Lee, D.M., D.S. Friend, M.F. Gurish, C. Benoist, D. Mathis, and M.B. Brenner. 2002. Mast cells: a cellular link between autoantibodies and inflammatory arthritis. *Science.* 297:1689–1692.
53. Secor, V.H., W.E. Secor, C.A. Gutekunst, and M.A. Brown. 2000. Mast cells are essential for early onset and severe disease in a murine model of multiple sclerosis. *J. Exp. Med.* 191:813–822.
54. Araki, Y., A. Andoh, Y. Fujiyama, and T. Bamba. 2000. Development of dextran sulphate sodium-induced experimental colitis is suppressed in genetically mast cell-deficient Ws/Ws rats. *Clin. Exp. Immunol.* 119:264–269.
55. Gregory, G.D., S.S. Raju, S. Winandy, and M.A. Brown. 2006. Mast cell IL-4 expression is regulated by Ikaros and influences encephalitogenic Th1 responses in EAE. *J. Clin. Invest.* 116:1327–1336.
56. Baumgartner, R.A., K. Ozawa, J.R. Cunha-Melo, K. Yamada, F. Gusovsky, and M.A. Beaven. 1994. Studies with transfected and permeabilized RBL-2H3 cells reveal unique inhibitory properties of protein kinase C gamma. *Mol. Biol. Cell.* 5:475–484.
57. Karin, M., and Y. Ben-Neriah. 2000. Phosphorylation meets ubiquitination: the control of NF-[kappa]B activity. *Annu. Rev. Immunol.* 18:621–663.
58. Nechushtan, H., M. Leitges, C. Cohen, G. Kay, and E. Razin. 2000. Inhibition of degranulation and interleukin-6 production in mast cells derived from mice deficient in protein kinase Cbeta. *Blood.* 95:1752–1757.
59. Zalewski, P.D., I.J. Forbes, C. Giannakis, P.A. Cowled, and W.H. Betts. 1990. Synergy between zinc and phorbol ester in translocation of protein kinase C to cytoskeleton. *FEBS Lett.* 273:131–134.
60. Forbes, I.J., P.D. Zalewski, C. Giannakis, and W.H. Betts. 1990. Zinc induces specific association of PKC with membrane cytoskeleton. *Biochem. Int.* 22:741–748.
61. Forbes, I.J., P.D. Zalewski, and C. Giannakis. 1991. Role for zinc in a cellular response mediated by protein kinase C in human B lymphocytes. *Exp. Cell Res.* 195:224–229.
62. Suzuki, T., K. Ishihara, H. Migaki, K. Ishihara, M. Nagao, Y. Yamaguchi-Iwai, and T. Kambe. 2005. Two different zinc transport complexes of cation diffusion facilitator proteins localized in the secretory pathway operate to activate alkaline phosphatases in vertebrate cells. *J. Biol. Chem.* 280:30956–30962.
63. Nishida, K., L. Wang, E. Morii, S.J. Park, M. Narimatsu, S. Itoh, S. Yamasaki, M. Fujishima, K. Ishihara, M. Hibi, et al. 2002. Requirement of Gab2 for mast cell development and KitL/c-Kit signaling. *Blood.* 99:1866–1869.
64. Nishida, K., S. Yamasaki, Y. Ito, K. Kabu, K. Hattori, T. Tezuka, H. Nishizumi, D. Kitamura, R. Goitsuka, R.S. Geha, et al. 2005. FcεRI-mediated mast cell degranulation requires calcium-independent microtubule-dependent translocation of granules to the plasma membrane. *J. Cell Biol.* 170:115–126.
65. Haase, H., S. Hebel, G. Engelhardt, and L. Rink. 2006. Flow cytometric measurement of labile zinc in peripheral blood mononuclear cells. *Anal. Biochem.* 352:222–230.